



저작자표시-비영리-변경금지 2.0 대한민국

이용자는 아래의 조건을 따르는 경우에 한하여 자유롭게

- 이 저작물을 복제, 배포, 전송, 전시, 공연 및 방송할 수 있습니다.

다음과 같은 조건을 따라야 합니다:



저작자표시. 귀하는 원저작자를 표시하여야 합니다.



비영리. 귀하는 이 저작물을 영리 목적으로 이용할 수 없습니다.



변경금지. 귀하는 이 저작물을 개작, 변형 또는 가공할 수 없습니다.

- 귀하는, 이 저작물의 재이용이나 배포의 경우, 이 저작물에 적용된 이용허락조건을 명확하게 나타내어야 합니다.
- 저작권자로부터 별도의 허가를 받으면 이러한 조건들은 적용되지 않습니다.

저작권법에 따른 이용자의 권리는 위의 내용에 의하여 영향을 받지 않습니다.

이것은 [이용허락규약\(Legal Code\)](#)을 이해하기 쉽게 요약한 것입니다.

[Disclaimer](#)

Adaptation of locomotion after nerve ablation of the medial gastrocnemius in young, non-disabled adults

Dongho Park

Department of Medicine

The Graduate School, Yonsei University

Adaptation of locomotion after nerve
ablation of the medial gastrocnemius in
young, non-disabled adults

Dongho Park

Department of Medicine

The Graduate School, Yonsei University

Adaptation of locomotion after nerve ablation of the medial gastrocnemius in young, non-disabled adults

Directed by Professor Dong-wook Rha

The Master's Thesis
submitted to the Department of Medicine,
the Graduate School of Yonsei University
in partial fulfillment of the requirements for the degree
of Master of Medical Science

Dongho Park

Dec 2020

This certifies that the Master's Thesis of
Dongho Park is approved.

Thesis Supervisor: Jung Hyun Park

Thesis Committee Member#1: Dong-wook Rha

Thesis Committee Member#2: Kyoungchul Kong

The Graduate School
Yonsei University

Dec 2020

ACKNOWLEDGEMENTS

First of all, it would not have been possible to write this thesis without the help and support of the kind people around me.

I would like to express my deep and sincere gratitude to my advisor Prof. Dong-wook Rha for the continuous support of my master's study and related research and for his patience, motivation, and immense knowledge. His guidance helped me throughout researching and writing this thesis. I could not have imagined having a better advisor and mentor for my master's study.

My appreciation also extends to my committee members, Prof. Kyoungchul Kong and Prof. Jung Hyun Park, who advised me with their insightful comments and encouragement. I am thankful for their hard questions that led me to widen my research from various perspectives.

<TABLE OF CONTENTS>

ABSTRACT.....	1
I. INTRODUCTION	3
II. MATERIALS AND METHODS	6
1. Experimental study.....	6
2. Musculoskeletal simulation.....	9
III. RESULTS	17
1. Experimental study.....	17
2. Musculoskeletal simulation.....	21
IV. DISCUSSION	29
V. CONCLUSION	36
REFERENCES	37
ABSTRACT (IN KOREAN)	42
PUBLICATION LIST	44

LIST OF FIGURES

Figure 1. Experimental study protocol.....	6
Figure 2. Comparing observation factors	10
Figure 3. Hill-type muscle-tendon model	11
Figure 4. Musculoskeletal model for walking.....	12
Figure 5. Examples of experimental EMG results.....	13
Figure 6. Muscle reflex scheme	14
Figure 7. Optimization framework	15
Figure 8. Changes in gait kinematics during level walking ...	17
Figure 9. Changes in linear enveloped muscle activity during level walking after medial GCM nerve ablation	18
Figure 10. Changes in gait kinematics during stair ascent ...	19
Figure 11. Changes in linear enveloped muscle activity during stair ascent after medial GCM nerve ablation.....	20
Figure 12. Comparing muscle activities according to J	22
Figure 13. Comparing muscle activities according to the models in the simulation	24
Figure 14. Gait kinematics when using an intact model and setting J as J_{cot} and $J_{fatigue}$	26
Figure 15. Gait kinematics when using a medial GCM paralyzed model and setting J as $J_{fatigue}$	28

LIST OF TABLES

Table 1. Kinematic data abbreviations.....	7
--	---

ABSTRACT

Adaptation of locomotion after nerve ablation of the medial gastrocnemius in young, non-disabled adults

Dongho Park

Department of Medicine

The Graduate School, Yonsei University

(Directed by Professor Dong-wook Rha)

Previous studies analyzed the activity of the gastrocnemius (GCM) medial and lateral heads as a single unit because it is technically challenging to separately analyze each component *in vivo*. However, functional variation between the medial and lateral heads is expected due to their anatomical differences.

To investigate the independent function of the GCM medial head, changes in gait kinematics and lower-limb muscle activities during level and stair ascent movements were analyzed in experimental and musculoskeletal predictive simulation studies following neurolysis of the tibial nerve branch, which innervates the medial head of the GCM.

During level walking, decreased GCM medial head activity did not significantly change gait kinematics. However, a significant increase in GCM

lateral head and hamstring activities occurred after a branch nerve block to the GCM medial head. During stair ascent, changes in surface electromyography activity only occurred in the GCM medial head, and post-procedure ankle dorsiflexion angles were significantly increased at the end of the terminal-stance phase. Ankle plantarflexion angles during the push-off phase were also decreased compared with pre-procedure values.

The results of the thesis suggest that the human body response to dysfunction of the GCM medial head depends on the type of locomotion.

Keywords: gastrocnemius, gait adaptation, gait analysis, predictive simulation, musculoskeletal model

**Adaptation of locomotion after nerve ablation of the medial
gastrocnemius in young, non-pathological adults**

Dongho Park

Department of Medicine

The Graduate School, Yonsei University

(Directed by Professor Dong-wook Rha)

I. INTRODUCTION

Locomotion is an important means for humans to move through places. The gastrocnemius (GCM) muscle plays a vital role in human locomotion including walking, stair climbing, and running. It generally engages in both ankle plantar and knee flexion and also acts to extend the knee during the stance phase of gait. The GCM comprises the medial and lateral heads and is connected to the calcaneus of the heel by a common tendon, the Achilles, which is shared with the soleus. The GCM and soleus account for 93% of theoretical plantar flexion torque.¹ In contrast to the GCM, the soleus is an uni-articular muscle that runs from the posterior surface of the tibia and fibula to the Achilles tendon.

During normal gait, the soleus initiates muscle activity during the latter part of

the loading response phase that continues until the terminal-stance phase ends. The GCM is a bi-articular muscle that originates from the medial and lateral condyles of the femur.

Within the GCM, functional discrepancies between the medial and lateral heads exist due to their different anatomical locations in the lower leg and structural characteristics including muscle thickness, fascicle length, and pennation angle. The lateral head has a smaller pennation angle, and the individual muscle fibers of the lateral head are 46% longer than the medial head muscle fibers.²⁻⁴

Previous studies have investigated the function of the medial and lateral heads of the GCM as a single unit because it is technically challenging to separately scrutinize these structures *in vivo*. Discriminating functional loss of each head due to injury or disease is rarely reported.⁵ To investigate the independent function of the GCM medial head, changes in gait kinematics and lower-limb muscle activities during level and stair ascent movements were analyzed following neurolysis of the tibial nerve branch, which supplies the medial head of the GCM.

A musculoskeletal simulative study was also conducted. Musculoskeletal simulation allows the independent cause of pathology to be investigated by freely setting an independent etiology that is challenging to study *in vivo* using a verified musculoskeletal model in a physical-based simulative environment. It is also possible to optimize the walking pattern adapted to the desired strategy by changing the cost function.

Musculoskeletal simulation allows the researcher to apply independent pathologies such as muscle weakness and joint contracture in a model of the

human body's muscles, ligaments, and bones in a virtual environment. The gait pattern caused by this pathology was predicted through forward simulation, and the results after treatment and surgery were also predicted. Validity has been demonstrated by comparing the predicted results of optimization-based simulation using musculoskeletal models with actual clinical results.⁶⁻⁸ For example, an optimization framework (SCONE) and a musculoskeletal framework can generate new motions to understand gait adaptation due to muscle deterioration and contracture of the triceps surae. Models have been created and verified.⁹ The controller that generates motion for walking follows the muscle reflex-based controller,¹⁰ the parameters of which are iteratively updated within the optimization framework. The simulation results in the intact model showed a similar walking pattern to the experimental results, and the predicted gait adaptation pattern for the paralyzed triceps surae model had a slower walking speed than the intact model in simulation.⁹

In a previous musculoskeletal simulative study, the model and gait controller verified during optimization-based simulation were modeled by combining the GCM medial and lateral head into one muscle for computational efficiency. To adequately reflect human body characteristics with GCM medial head paralysis, it is necessary to develop and verify the musculoskeletal model with separated medial and lateral heads of the GCM and the corresponding gait controller.

This study aimed to investigate the independent function of the GCM medial head by conducting experimental and musculoskeletal simulative studies following the neurolysis of the tibial nerve branch that supplies the GCM medial head.

II. MATERIALS AND METHODS

1. Experimental study

A. Participants

The study group included 12 non-disabled adults (2 males and 10 females; age: 28.2 [\pm 7.72] years; height: 162.44 [\pm 5.04] cm, mass: 57.31 [\pm 7.07] kg) who were scheduled to undergo neurolysis of the tibial nerve branch for aesthetic calf reduction using 400-kHz radiofrequency nerve ablation. Subjects with a previous history of lower extremity orthopedic surgery or other problems that affect typical gait pattern were excluded.

B. Protocol

Three-dimensional gait analysis and surface electromyography (EMG) were performed before tibial nerve branch ablation and 1 week and 3 months after the operation (Fig. 1).

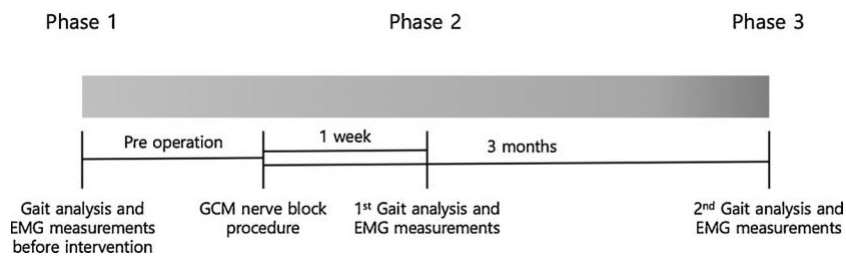


Fig. 1. Experimental study protocol.

C. Gait analysis

Gait analysis was performed using a computerized optoelectric gait analysis system (VICON MX-T10 Motion Analysis System, Oxford Metrics Inc., Oxford, UK; sampling frequency 100 Hz) to measure gait kinematics. Sixteen reflective markers were attached to the subject's body according to the VICON Plug-in-Gait model guidelines. Data were collected while subjects walked at a comfortable, self-selected speed on an 8-m pathway. The following parameters were analyzed to compare kinematic data (Table 1).

Table 1. Kinematic data abbreviations.

<i>Joint</i>	<i>Key (°)</i>	<i>Description</i>
Ankle	ASA1	Ankle dorsiflexion angle at initial contact
	ASA2	Ankle maximum dorsiflexion angle during the stance phase
	ASA3	Ankle maximum plantar flexion angle during push-off
	ASA4	Ankle dorsiflexion angle at the end of the terminal swing
	ATA1	Ankle internal rotation angle at initial contact
	ATA2	Ankle maximum internal rotation angle during the stance phase
	ATA3	Ankle maximum external rotation angle during the swing phase
	ATA4	Ankle internal rotation angle at the end of the terminal swing
Knee	KSA1	Knee flexion angle at initial contact
	KSA2	Knee minimum flexion angle during the stance phase
	KSA3	Knee maximum flexion angle during the swing phase
	KSA4	Knee flexion angle at the end of the terminal swing
Hip	HSA1	Hip flexion angle at initial contact
	HSA2	Hip maximum extension angle during the stance phase
	HSA3	Hip flexion angle at the end of the terminal swing
	HCA1	Hip adduction angle at initial contact
	HCA2	Hip max adduction angle during the stance phase
	HCA3	Hip adduction angle at the end of the terminal swing

D. Electromyography (EMG) measurements

Surface EMG (MA300-XVI, Motion lab systems, USA; sampling frequency 1000 Hz) was simultaneously recorded with the gait analysis. Surface electrodes were placed on the peroneus longus, medial hamstring, tibialis anterior, vastus medialis, soleus, and medial and lateral heads of the GCM according to SENIAM guidelines.¹¹ Ultrasonography (Accuvix V10c system; Samsung Medison Co., Seoul, South Korea) was used to confirm correct electrode placement. Data were filtered by a 10- to 500-Hz band-pass filter and time-normalized by dividing 1 gait cycle into 16 equally spaced intervals. Root mean square (RMS) values were calculated for individual muscles during each time interval. Pre- and post-procedure RMS values for each muscle were expressed as a ratio of the maximum pre-procedure RMS value.¹² All data were averaged for three left and three right gait cycles.

E. Operation

The shape and contour of the medial head of the GCM were inspected while the subjects stood on tiptoe to induce maximum muscle contraction. Ultrasonography in the prone position was used to identify nerve and vessel locations in the popliteal fossa and calf areas. The muscle margins and nerve locations were marked with a surgical pen. After administration of local anesthesia using 1% lidocaine, a radiofrequency (RF) probe connected to a 400-kHz-electrical surgical unit (ITC-300D, ITC Co., South Korea) was inserted through a small skin incision below the popliteal crease. The motor nerve branches that supplied the medial GCM were ablated using an electrical

stimulator to transmit RF energy. Insulation of the RF probe (except for the needle tip) enabled precise ablation of nerve branches with minimal injury to adjacent tissues. To confirm procedure success, leg shape was visually inspected at the first post-operative visit. The procedure was considered successful when the maximum EMG value decreased to at least 30% of the maximum pre-operative value.

F. Statistical analysis

Pre-procedure and 1-week and 3-month post-procedure data were compared using a linear mixed model. Two-sided p -values < 0.05 were considered statistically significant.

2. Musculoskeletal simulation

A. Observation factors

(1) Muscle activity (Exp-EMG) and gait kinematics (Exp-KM) during normal walking in the experimental study, and muscle activity (Sim-EMG) and gait kinematics (Sim-KM) during normal walking in the predictive simulation using an objective function that minimizes the Cost of Transportation (J_{cot}).

(2) Muscle activity (Exp-EMG) and gait kinematics (Exp-KM) during normal walking in the experimental study, and muscle activity (Sim-EMG) and gait kinematics (Sim-KM) during normal walking in the predictive simulation using an objective function that minimizes the fatigue ($J_{fatigue}$) (Fig. 2).

(3) Muscle activity (Exp-block-EMG) and gait kinematics (Exp-block-KM) during medial GCM paralyzed walking in the experimental study, and muscle activity (Sim-block-EMG) and gait kinematics (Sim-block-KM) during medial GCM paralyzed walking in the predictive simulation using an objective function that minimizes the Cost of Transportation (J_{cot}).

(4) Muscle activity (Exp-block-EMG) and gait kinematics (Exp-block-KM) during medial GCM paralyzed walking in the experimental study, and muscle activity (Sim-block-EMG) and gait kinematics (Sim-block-KM) during medial GCM paralyzed walking in the predictive simulation using an objective function that minimizes the fatigue ($J_{fatigue}$) (2.D (p. 15)) (Fig. 2).

Root Mean Squared Error (RMSE)	
• J_{cot}	• J_{cot}
• $J_{fatigue}$	• $J_{fatigue}$
Sim-EMG <-> Exp-EMG	Sim-block-EMG <-> Exp-block-EMG
Sim-KM <-> Exp-KM	Sim-block-KM <-> Exp-block-KM

Fig. 2. Comparing observation factors.

B. Musculoskeletal model

The musculoskeletal model used in this study is a planar model based on previously described lower extremity model.¹³ This model has 9 degrees of freedom: pelvis, 3 degrees of freedom (translation); hip, 1 degree of freedom in rotational motion in the sagittal plane (hip flexion/extension); ankle, 1 degree of freedom in rotational motion in the sagittal plane (dorsi/plantar flexion); and knee joints, 1 degree of freedom (knee flexion/extension) combined with rotation and translation in the sagittal plane.

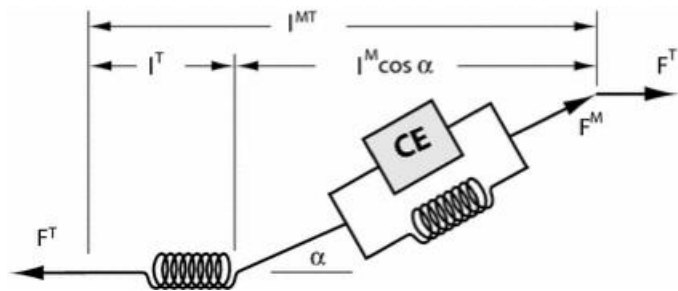


Fig. 3. Hill-type muscle-tendon model.

This model is a single muscle-tendon unit that combines the peak-isometric force of each muscle with similar function in the sagittal plane using a Hill-type muscle-tendon unit¹⁴ gluteus maximus, iliopsoas, vastus medialis, hamstrings, GCM medial and lateral heads, soleus, and tibialis anterior (Fig. 3). The highest isometric contractile force is based on previous musculoskeletal models.¹⁵ Tendon deformity at the maximum isometric contractile force is set to 4.9%¹⁵ for all muscles except the plantar flexors, which are set to 10%.

The ligament is modeled as a non-linear rotating spring to generate torque when the joint is overly flexed or extended. In this model, the ligaments generate torque when the hips are bent over 120° or stretched over 30° . Torque is generated when the knee is bent over 140° or extended over 0° , and the ankle is dorsiflexion above 20° or plantarflexion above 40° .

A compliant contact model¹⁶ is used to generate a force between the foot and ground. There are three contact spheres on each foot: one sphere with a radius of 5 cm represents the heel, and two spheres with radii of 2.5 cm represent the first and fifth metatarsophalangeal joints (Fig. 4).

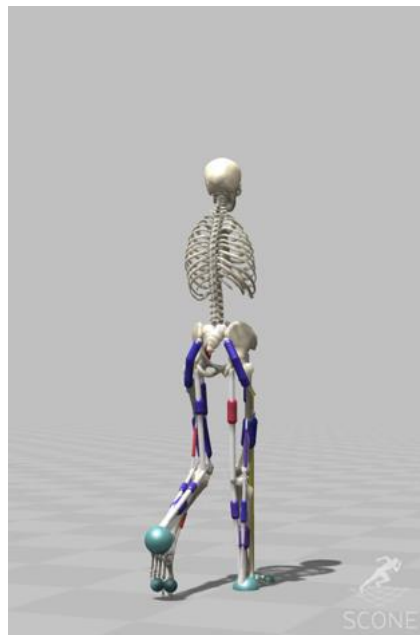


Fig. 4. Musculoskeletal model for walking.

The maximum isometric contractile force of the muscles in the model with the paralyzed GCM medial head was set at 25% of the maximum force of the intact model by referring to the existing experimental data (Fig. 5).

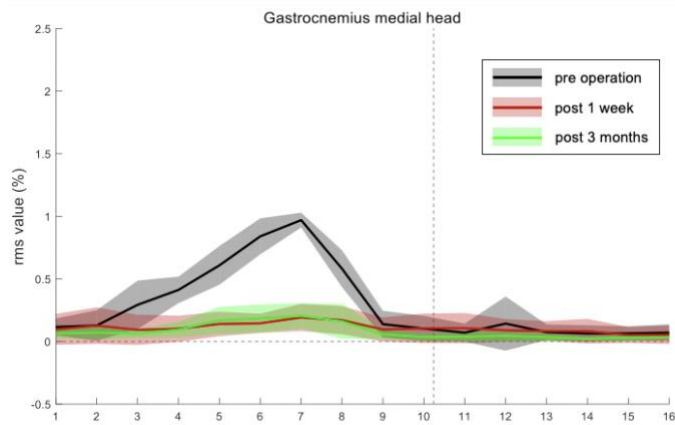


Fig. 5. Examples of experimental EMG results.

C. Gait controller

The gait controller is based on a muscle reflex-based controller that is widely used to generate human gait in predictive simulation.¹⁷⁻¹⁹ The walking cycle of each leg is divided into five stages that can be controlled: early stance phase (ES), mid-stance phase (MS), pre-swing phase (PS), swing phase (S), and weight preparation phase (Landing preparation phase, LP)¹⁸ (Fig. 6).

	Stance			Swing	
	<i>ES</i>	<i>MS</i>	<i>PS</i>	<i>S</i>	<i>LP</i>
AII	C		C	C	
GMAX	L+, V+, PD			L+	
HAMS	L+, V+, PD			L+	
ILPSO	PD		L+	L+	L+
RF	L+				
VAS	L+, V+			L+	
BFSH				L+	
GAS	F+				
SOL	F+				
TA	L+			L+	L+
	F ⁻ (SOL)				

Fig. 6. Muscle reflex scheme.

D. Optimization framework

To evaluate the optimization parameters, the objective function was defined as J , and optimization was performed to minimize this variable (Fig. 7).^{9, 20}

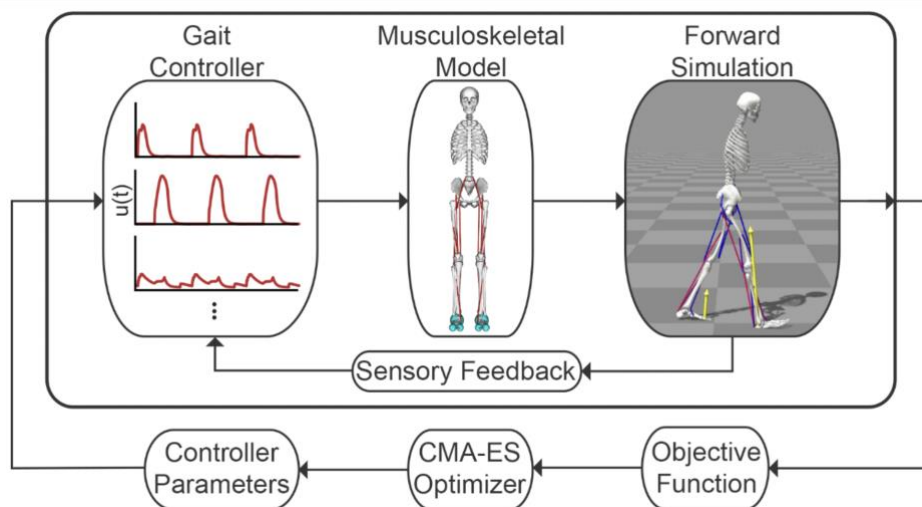


Fig. 7. Optimization framework⁹

$$J1 = J_{cot} + w_{speed} * J_{speed} + w_{injury} * J_{injury} + w_{head} * J_{head}$$

$$J2 = J_{fatigue} + w_{speed} * J_{speed} + w_{injury} * J_{injury} + w_{head} * J_{head}$$

The goal of optimization was to maintain a prescribed walking speed, avoid falls (J_{speed}), avoid ligament injuries (J_{injury}), and stabilize the head (J_{head}). To balance the objective function, the weights were fixed to $w_{speed} = 10,000$, $w_{injury} = 0.1$ and $w_{head} = 0.25$ according to a previous study.⁹ The simulation was also optimized for the purpose of minimizing the cost of transportation (J_{cot}) or muscle fatigue ($J_{fatigue}$).

J_{cot} penalized the simulation when the model walked in a metabolically less efficient manner, which was calculated by summing the metabolic rate per muscle to estimate the total metabolic rate (E) during the simulation period. It was normalized by body weight (m) and travel distance (d).

$$J_{cot} = \sum E * (md)^{-1}$$

$J_{fatigue}$ penalized the simulation of walking in a way that builds muscle fatigue and sums the squares of the activities of all muscles to calculate their fatigue during the simulation.

$$J_{fatigue} = \sum \text{muscle activation}^2$$

III. RESULTS

1. Experimental study

A. Level walking

All kinematic data of the ankle, knee, and hip joints in the sagittal, coronal, and transverse planes revealed statistically insignificant changes after ablation of the tibial nerve branch innervating the GCM medial head (Fig. 8).

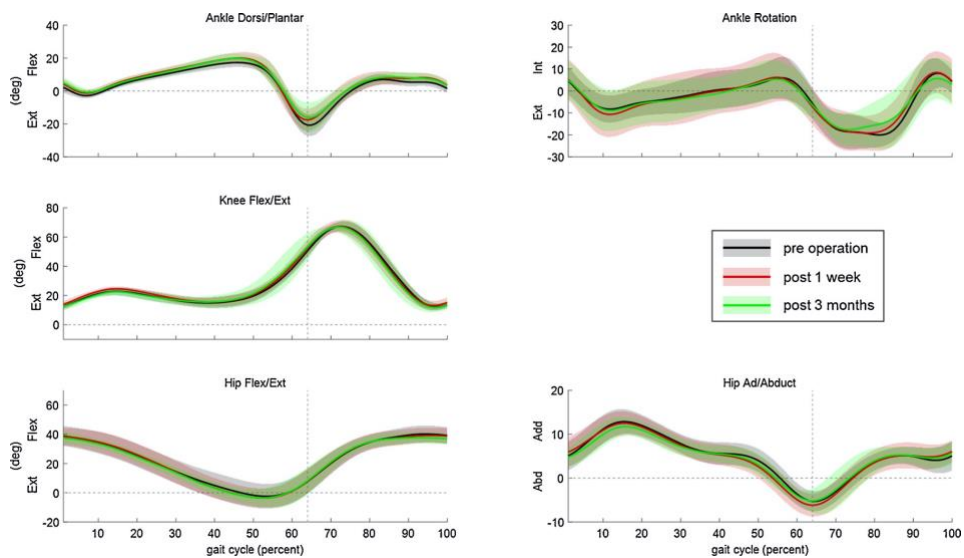


Fig. 8. Changes in gait kinematics during level walking. Vertical dashed lines divide the stance and swing phases of the gait cycle.

The RMS values of the GCM medial head during the mid-stance phase significantly decreased after the procedure compared with pre-procedure values ($p<0.01$). In contrast, the GCM lateral head's RMS values in this phase significantly increased after the procedure compared with pre-procedure values ($p<0.01$). The hamstring muscle also showed a statistically significant increase in RMS values during the procedure ($p<0.05$) (Fig. 9).

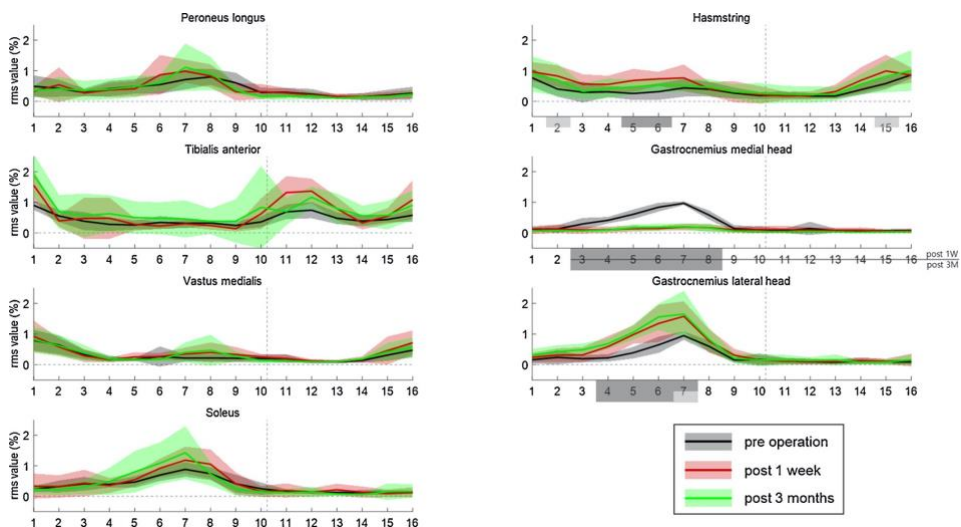


Fig. 9. Changes in linear enveloped muscle activity during level walking after medial GCM nerve ablation. Dark and light gray areas of the x-axis indicate $p<0.01$ and $p<0.05$, respectively.

B. Stair ascent

Angle joint kinematics during stair climbing showed statistically significant changes. Post-procedure ankle dorsiflexion angles at the end of the terminal-stance phase (ASA2) increased $3.29^\circ (\pm 0.82)$ 1 week after the procedure compared with the pre-procedure value ($p=0.007$). At 3 months post-procedure, the ankle dorsiflexion angle had increased at $4.36^\circ (\pm 1.18)$ compared with baseline ($p=0.015$). The ankle plantarflexion angle during the push-off phase (ASA3) measured 1 week after ablation also significantly decreased by $9.51^\circ (\pm 1.60)$ compared with pre-procedure values ($p<0.01$). Furthermore, at the 3-month follow-up, ankle plantarflexion had decreased $6.93^\circ (\pm 1.36)$ compared with baseline ($p<0.01$) (Fig. 10).

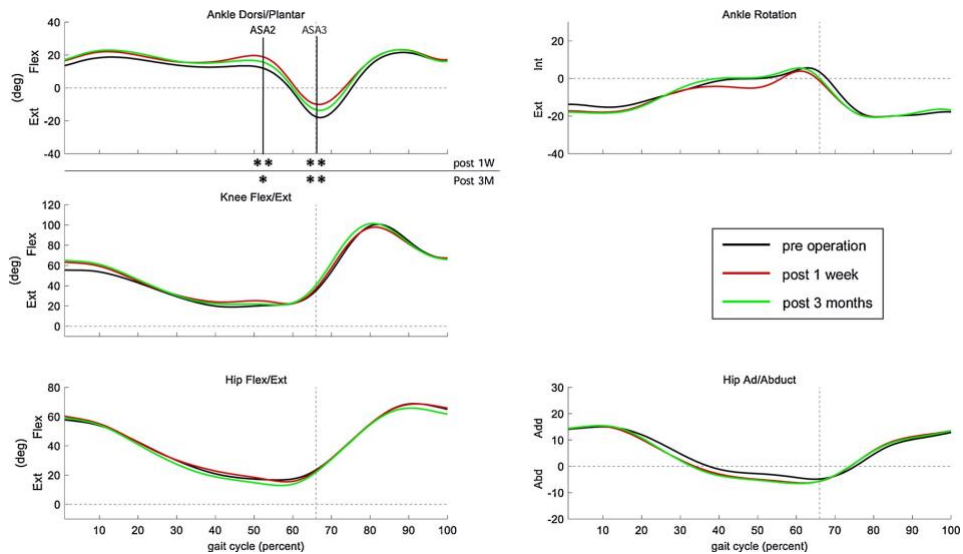


Fig. 10. Changes in gait kinematics during stair ascent. * $p<0.05$, ** $p<0.01$, linear mixed model.

Post-procedure RMS values of the GCM medial head during the mid-stance phase of the stair ascent were significantly decreased after the procedure ($p < 0.05$). However, EMG data from the remaining muscles revealed statistically insignificant changes during stair ascent (Fig. 11).

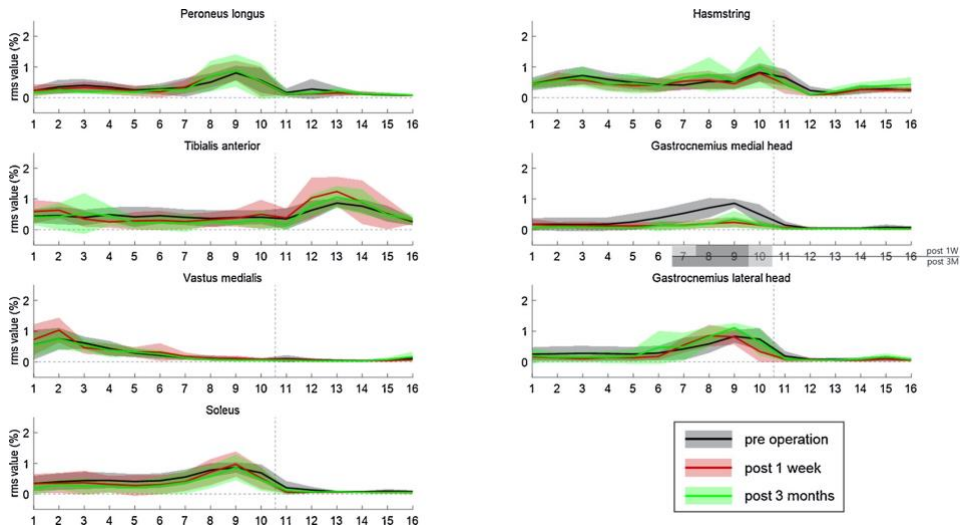


Fig. 11. Changes in linear enveloped muscle activity during stair ascent after medial GCM nerve ablation. Dark gray and light gray areas of the x-axis indicate $p < 0.01$ and $p < 0.05$, respectively.

2. Musculoskeletal simulation

A. Comparing Exp-EMG and Sim-EMG during gait according to the objective function (J).

(1) Objective function as J_{cot}

When J was set to J_{cot} , Sim-EMG showed a very different trend from Exp-EMG. The lateral GCM head was only initiated after the medial GCM head was saturated.

(2) Objective function as $J_{fatigue}$

On the other hand, when the objective function was set to $J_{fatigue}$, muscle activities of the GCM medial and lateral heads and soleus of Sim-EMG were evenly activated, showing a pattern very similar to Exp-EMG (Fig. 12).

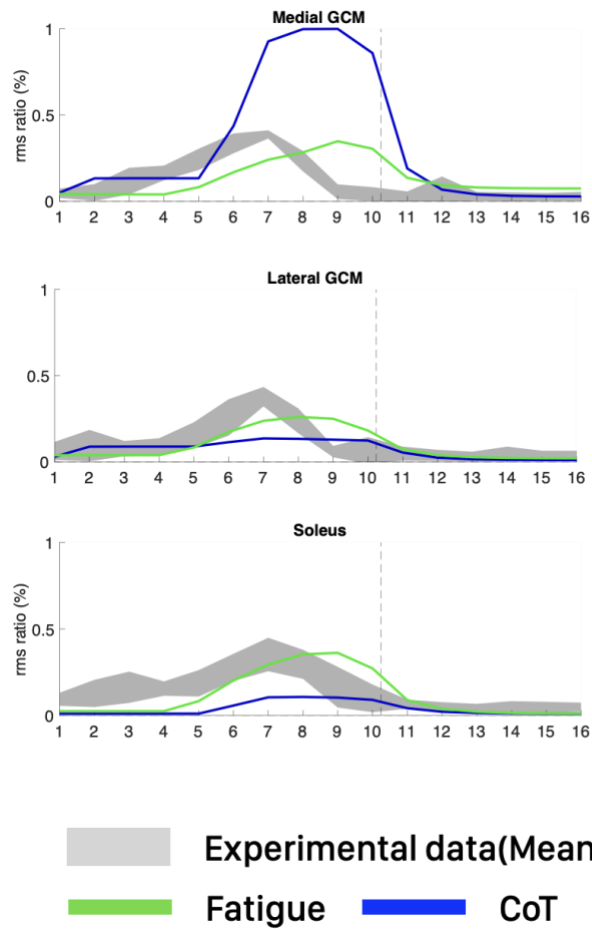


Fig. 12. Comparing muscle activities according to J . The solid blue and green lines represent setting an objective function as J_{cot} and $J_{fatigue}$, respectively. The gray shaded area indicates 2 SDs of the experimental normal gait data.

Since Sim-EMG showed similar results to Exp-EMG when J was set to J_{fatigue} , this was done to see the adaptation when the GCM medial head was paralyzed in the musculoskeletal model.

(3) Objective function as J_{fatigue}

As in the experimental data, GCM medial head muscle activity in Sim-block-EMG was decreased more than in Sim-EMG, GCM lateral head muscle activity in Sim-block-EMG was increased more than Sim-EMG, and muscle activity of the soleus of Sim-block-EMG was similar to that before GCM medial head paralysis in Sim-EMG (Fig. 13).

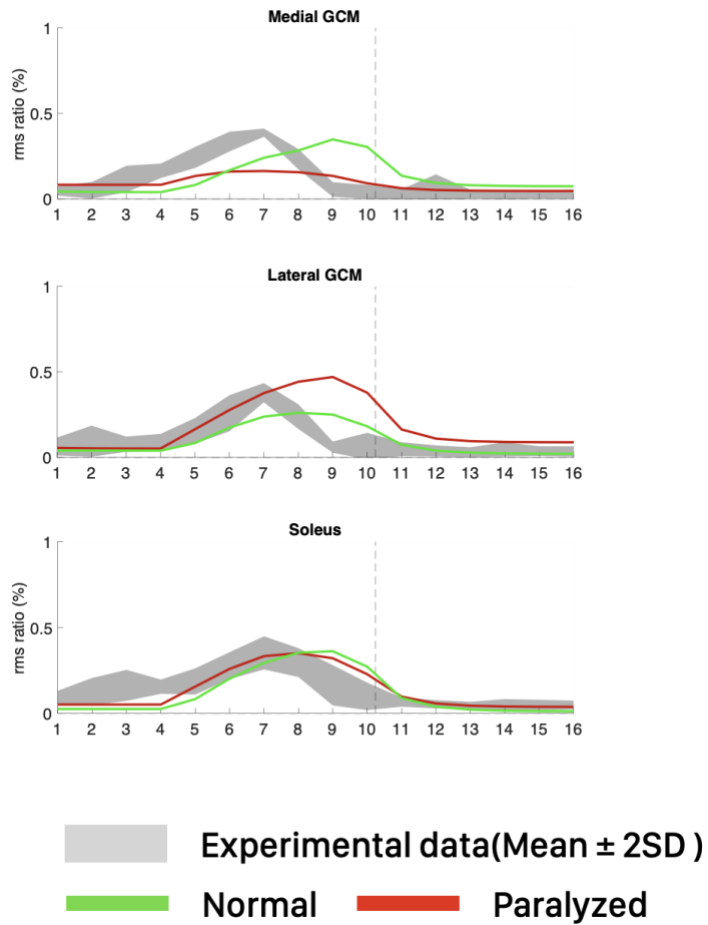


Fig. 13. Comparing muscle activities according to the models in the simulation. The solid green and red lines represent intact (Sim-EMG) and medial GCM paralyzed models (Sim-block-EMG), respectively. The gray shaded area indicates 2 SDs of the experimental normal gait data.

B. Comparing Sim-KM and Exp-KM according to the objective function

(J).

(1) Objective function as J_{cot}

Sim-KM had generally similar trends with Exp-KM when setting J as J_{cot} . Sim-KM were within 2 SDs for most of the gait cycle.

(2) Objective function as $J_{fatigue}$

The overall trends of Sim-KM when setting J to $J_{fatigue}$ were also similar to Exp-KM (Fig. 14).

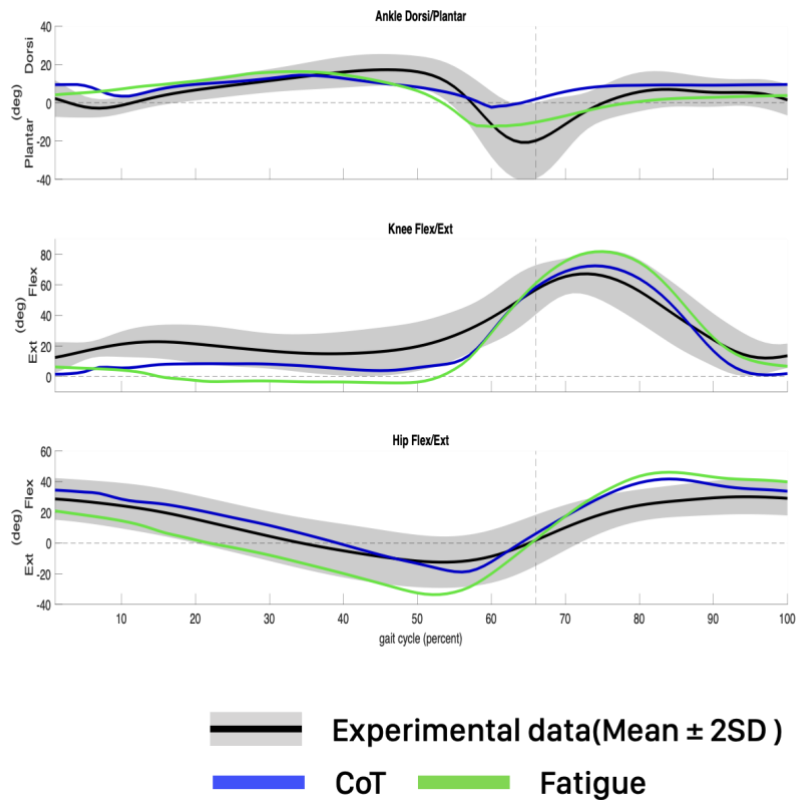


Fig. 14. Gait kinematics using an intact model and setting J as J_{cot} and $J_{fatigue}$. The solid black, blue, and green lines represent the mean value of Exp-KM, Sim-KM using J as J_{cot} , and Sim-KM using J as $J_{fatigue}$, respectively. The gray shaded area indicates 2 SDs of the experimental normal gait data.

The shape of the simulated trajectory when the objective function was set to J_{fatigue} and Sim-block-KM was generally similar to Exp-block-KM. For the majority of the gait cycle, Sim-block-KM were within 2 SDs of Exp-block-KM. Although the medial GCM was paralyzed, Sim-KM and Sim-block-KM using J as J_{fatigue} were almost similar (Fig. 15).

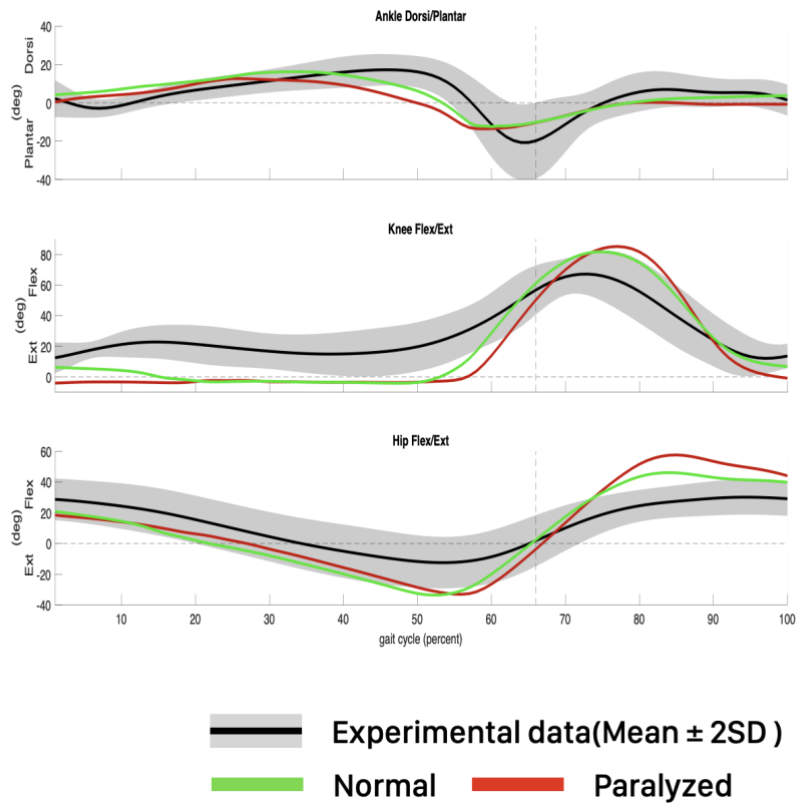


Fig. 15. Gait kinematics when using a medial GCM paralyzed model and setting J as J_{fatigue} . The solid black, green, and red lines represent the mean value of Exp-KM, Sim-KM, and Sim-block-KM, respectively. The gray shaded area indicates 2 SDs of the experimental normal gait data.

IV. DISCUSSION

The GCM medial head plays a vital role as the ankle plantar flexor during the terminal-stance and push-off phases. Therefore, we hypothesized that maximum ankle dorsiflexion would increase during the terminal-stance phase and that maximum ankle plantar flexion would decrease during the push-off phase due to GCM medial head paralysis. It was reported that ankle dorsiflexion and knee flexion increased in the stance phase during level walking after a tibial nerve block that paralyzed all ankle plantar flexors including the GCM, soleus, flexor hallucis longus, flexor digitorum longus, and tibialis posterior.⁵ In contrast to our hypothesis, decreased activity of the GCM medial head did not significantly change gait kinematics during level walking in our study. However, the GCM lateral head's activity significantly increased at 1 week and 3 months after nerve ablation to the GCM medial head. Hamstring activity was also significantly increased, but only at the 1-week post-procedure timepoint. The compensatory hyperactivities of other muscles might help maintain gait kinematics, which was unchanged during level walking after the procedure.

Human bipedal walking is known to be energy efficient, and proper kinematics of the lower extremities is essential for this energy efficiency.²¹⁻²³ During walking, the GCM plays a vital role beginning from the end of the loading response and extending to the terminal-stance phase. Dynamic stability is altered by continued realignment of the ground reaction force vector to the joints. Focusing on the ankle joint, the ground reaction force vector is located posterior to the ankle joint during the loading response. In mid-stance, the ground reaction force vector advances from the heel (posterior to the ankle joint) to the foot (anterior to the

ankle joint), responding to the momentum from the limb swing and bodyweight forward fall, to produce the dorsiflexion moment at the ankle joint. The ankle plantar flexors act to prevent rapid ankle dorsiflexion that decelerates the tibia's progression during this phase. These actions help to keep the ground reaction force vector anterior to the knee joint and maintain a straight leg without collapsing. By the end of mid-stance, the base of the body vector lies in the forefoot. With the ankle virtually locked by the plantar flexors, the heel rises as the tibia continues to advance.²⁴ In the terminal-stance, the vector at the metatarsal head initiates progression over the forefoot rocker. There is also a demand for the plantar-flexor activity to support the heel rise. The heel rise opposes the falling body weight and the dorsiflexor torque generated by the falling body weight.

This dynamic walking mechanism is based on an inverted pendulum theory, and the alignment of the lower limbs during walking is very important.²⁵⁻²⁷ Proper alignment of the lower extremities must be maintained to keep the positional relationship between the ground reaction force vector and the joint center, which allows for minimal muscle activity during walking. However, if the positional relationship is not maintained, energy consumption increases. In several studies of patients with cerebral palsy, the lower limbs' alignment was disrupted during crouch gait and caused some muscles to work more—the metabolic cost of walking increased, and eventually, knee pain and degeneration occurred.²⁸⁻³¹ Additionally, in the crouched posture, an increase in joint flexion acceleration, which is caused by gravity, and a decrease in the muscle capacity to produce joint extension accelerations, requires these individuals to produce larger muscle

forces to maintain the crouched posture.³² It is essential to maintain proper alignment of the lower limbs to achieve effective level walking.

Therefore, it appears the ankle plantar flexors play a crucial role in level walking efficiency. The hamstring that acts as a hip extensor contributes to upright trunk posture and limb stabilization around initial contact and contributes to knee extension during the stance phase.^{6,32} This result indicates that the GCM lateral head and hamstrings compensate for the GCM medial head to maintain gait kinematics during level walking.

On the stair ascent, there was a kinematic change during the stair ascent. Ankle dorsiflexion increased at the end of the terminal-stance phase (ASA2), and the maximum ankle plantarflexion angle (ASA3) decreased during push-off due to ankle plantar-flexor weakness. In contrast to level walking, compensatory hyperactivities in the GCM lateral head and hamstrings were not observed during stair ascent.

A striking feature of normal walking is the continued smooth, forward movement of the human body's center of mass (CoM). In addition, normal gait patterns are energy efficient and use the natural dynamics of the whole body. However, stair climbing movements are different than normal walking.³³⁻³⁶ These motions consume energy because they move the CoM upward and forward. Besides, when the magnitude of the forward acceleration is small, the deviation between the pressure center and zero-moment point is small, and the center of pressure is primarily in the support base. Additional voluntary knee flexion during the swing phase is also required to maintain foot clearance during a stair ascent. The most noticeable difference between stair climbing and level walking

is that knee extension during the stance phase is essential for moving the CoM upward. The knee joint movement from flexion to extension during the stance phase is considerable and requires the knee extensor muscles to produce a large extension torque and positive vertical power to move the upper body against gravity. Although the ankle joint is also plantarflexed during the mid-to terminal-stance phases, and the joint produces positive work, its role in moving the CoM upward is smaller than that during knee extension. In our study, ankle dorsiflexion during the terminal-stance phase increased, but knee kinematics during stair ascent were unchanged following nerve ablation. Conversely, during normal level walking, the knee extensors produced less torque, including negative power during most stance phases. The ankle plantar flexors produced greater torque to keep the ground reaction force vector anterior to the knee joint and maintain a straight leg without collapsing.

Because the pendulum model for level walking does not apply to stair climbing, proper kinematics that align the hip, knee, and ankle joints in a way that is appropriate for this model are less important. In addition, the higher muscular demand required for stair ascent may exacerbate the effects of weakness, making it more difficult to compensate and maintain normal kinematics. These reasons may explain why kinematics were only altered during the stair ascent and not during level walking after paralysis of the GCM medial head.

In the predictive simulation conducted for this thesis, it was necessary to modify the previously verified musculoskeletal model that combined the medial and lateral heads of the GCM into a single muscle. To build a model in which only the medial head was paralyzed, the GCM had to be separated into the medial

and lateral heads.

To verify the modified model, an optimization simulation was first performed using an objective function as the CoT (which is the most used and validated in previous predictive simulation studies) in the musculoskeletal model with separate medial and lateral heads. The resulting joint kinematics and muscle activity were subsequently verified with the experimental data.

Wang and colleagues reported a study of optimization simulations that create gait while minimizing the CoT of the musculoskeletal model. They showed that optimization function as the CoT produced gait kinematics and muscle activity much closer to humans than previous works.¹⁹ In Wang *et al.* and previous studies, the muscles moving one joint were simplified to one muscle, while the GCM muscles moving the knee and ankle joints were separated into medial and lateral heads in this study. At this point, an issue arises as to how two muscles with the same function to move the joint should be activated in harmony. When simulating using the objective function as the CoT, the gait kinematics showed a similar trend to the experimental results (Fig. 14). However, muscle activity showed a very different pattern from the experimental results. Unlike the experimental results in which the GCM medial and lateral heads are activated simultaneously, the GCM medial head was activated first in the simulation, and the lateral GCM muscle was only activated once the GCM medial head was saturated (Fig. 12).

In contrast to the CoT, several studies have reported that fatigue better reflects load sharing in musculoskeletal models. If two muscles contribute to one task, activating one muscle more than the other does not effectively influence energy

consumption. However, this does not happen if fatigue is used as the objective function.³⁷

When simulating fatigue as an objective function, both muscle activity and joint angles showed similar trends to normal walking in the experimental data. Accordingly, the simulation using the musculoskeletal model with redundant muscles suggests that the results of fatigue as the objective function show a more realistic muscle activity pattern (Fig. 12, 14).

Therefore, the objective function was set to fatigue to observe gait adaptation after medial GCM paralysis. The simulation findings were similar to the experimental results; medial GCM muscle activity decreased, gait kinematics did not show a significant change after paralysis, and gait adaptation showed increased activity of the lateral GCM muscle.

A more in-depth look at the nervous system level that controls locomotion provides some insight. Researchers have investigated the spinal cord for 100 years to decode how the human body generates locomotion. Most studies focused on specialized spinal circuits involved in the control of locomotor movement pattern generation and modulation. Experimental works performed over several decades concluded that walking, flying, and swimming are controlled by a network of spinal neurons commonly referred to as the central pattern generator (CPG).³⁸ There was early evidence and underlying notions of the CPG. Thomas Graham Brown studied this issue in the early 20th century and ultimately changed his view of neural control of locomotion.³⁹ It has been demonstrated that in all vertebrate species investigated from lampreys to humans, the CPG can self-produce, even under some conditions without descent or peripheral input,

basic rhythm and coordinated locomotion.⁴⁰ According to Philipson's observations, it was concluded that the spinal cord uses central and reflex mechanisms to control locomotion.⁴¹ Charles Sherrington's transection experiments in cats and dogs provided additional evidence that the result of these locomotor-like movements is proprioceptors' reflex action on some spinal centers.⁴²

Spinal reflexes also play a crucial role in controlling locomotion. While the CPG creates a rudimentary, stereotypical locomotion pattern, reflexes such as Ia and Ib play a role in tonus and postural adjustments, significantly enhance muscular contraction of extensors during the stance phase, and reset stepping to the extension when activated during the swing phase.⁴³⁻⁴⁷ This reflex input to the CPG compensates for the unexpected increase in limbs during walking but can also increase extensor muscle tonus during the posture. In other words, the CPG acts as a feedforward that generates basic locomotion patterns, and the spinal reflex serves as feedback that adapts to external environments or changes. However, it is not known precisely what proportions of the CPG and spinal reflex act during walking.

When the medial GCM muscle—one of the main plantar flexors—was paralyzed, the lateral GCM muscle was recruited more instead of decreasing the ankle flexion angle. This compensation maintained gait kinematics and was similar in both clinical trials and neuromuscular simulations. It could be inferred that the human body uses a compensation strategy based on a feedback mechanism when the medial flexor muscle is paralyzed when walking on level ground.

V. CONCLUSION

This study investigated level walking and stair ascent, and the results revealed that the human body differentially compensated for GCM medial head dysfunction depending on the type of locomotion. Specifically, the muscles around the medial GCM became more active during level walking and showed gait adaptation to maintain the kinematic pattern. Gait adaptation also occurred during stair ascension; the surrounding muscles do not hyperactivate, and the kinematic pattern changes.

The results also suggest that when comparing muscle activity in an optimization-based simulation using a musculoskeletal model with redundant muscles, setting Fatigue as an objective function rather than Cost of Transportation more realistically reflects the physiology of the actual human body.

REFERENCES

1. Haxton HA. Absolute muscle force in the ankle flexors of man. *The Journal of Physiology*. 1944;103(3):267-73.
2. Antonios T, Adds PJ. The medial and lateral bellies of gastrocnemius: a cadaveric and ultrasound investigation. *Clinical Anatomy*. 2008;21(1):66-74.
3. Park ES, Sim E, Rha D, Jung S. Architectural changes of the gastrocnemius muscle after botulinum toxin type A injection in children with cerebral palsy. *Yonsei Medical Journal*. 2014;55(5):1406-12.
4. Riemann BL, Limbaugh GK, Eitner JD, LeFavi RG. Medial and lateral gastrocnemius activation differences during heel-raise exercise with three different foot positions. *Journal of Strength & Conditioning Research*. 2011;25(3):634-9.
5. Sutherland DH, Cooper L, Daniel D. The role of the ankle plantar flexors in normal walking. *Journal of bone and joint surgery American volume*. 1980;62(3):354-63.
6. Steele KM, Seth A, Hicks JL, Schwartz MS, Delp SL. Muscle contributions to support and progression during single-limb stance in crouch gait. *J Biomech*. 2010 2010/08//;43(11):2099-105.
7. Steele KM, van der Krogt MM, Schwartz MH, Delp SL. How much muscle strength is required to walk in a crouch gait? *J Biomech*. 2012;45(15):2564-9.
8. van der Krogt MM, Bar On L, Kindt T, Desloovere K, Harlaar J. Neuro-musculoskeletal simulation of instrumented contracture and spasticity assessment in children with cerebral palsy. *Journal of NeuroEngineering and Rehabilitation*. 2016;13(1):64-.
9. Ong CF, Geijtenbeek T, Hicks JL, Delp SL. Predicting gait adaptations due to ankle plantarflexor muscle weakness and contracture using physics-based musculoskeletal simulations. *PLoS Computational Biology*. 2019;15(10):e1006993-e.

10. Park D, Seong YJ, Woo H, Yoo B, Shim D, Kim ES, et al. Paralysis of the gastrocnemius medial head differentially affects gait patterns and muscle activity during level and stair ascent locomotion. *Gait Posture*. 2019 Jul;72:222-7.
11. Hermens HJ, Freriks B, Disselhorst Klug C, Rau G. Development of recommendations for SEMG sensors and sensor placement procedures. *Journal of electromyography and kinesiology*. 2000;10(5):361-74.
12. Romkes J, Hell AK, Brunner R. Changes in muscle activity in children with hemiplegic cerebral palsy while walking with and without ankle-foot orthoses. *Gait & posture*. 2006;24(4):467-74.
13. Delp SL, Loan JP, Hoy MG, Zajac FE, Topp EL, Rosen JM. An interactive graphics-based model of the lower extremity to study orthopaedic surgical procedures. *IEEE Transactions on Biomedical Engineering*. 1990;37(8):757-67.
14. Thelen DG. Adjustment of muscle mechanics model parameters to simulate dynamic contractions in older adults. *Journal of Biomechanical Engineering*. 2003;125(1):70-7.
15. Rajagopal A, Dembia CL, DeMers MS, Delp D, Hicks JL, Delp SL. Full-Body Musculoskeletal Model for Muscle-Driven Simulation of Human Gait. *IEEE Transactions on Biomedical Engineering*. 2016;63(10):2068-79.
16. Hunt KH, Crossley FRE. Coefficient of Restitution Interpreted as Damping in Vibroimpact. *Journal of Applied Mechanics*. 1975;42(2):440-5.
17. Dorn TW, Wang JM, Hicks JL, Delp SL. Predictive simulation generates human adaptations during loaded and inclined walking. *PLoS ONE*. 2015;10(4):e0121407-e.
18. Geyer H, Herr H. A muscle-reflex model that encodes principles of legged mechanics produces human walking dynamics and muscle activities. *IEEE Transactions on Neural Systems and Rehabilitation Engineering*. 2010;18(3):263-73.

19. Wang JM, Hamner SR, Delp SL, Koltun V. Optimizing Locomotion Controllers Using Biologically-Based Actuators and Objectives. *ACM Transactions on Graphics (TOG)*. 2012;31(4).
20. Song S, Geyer H. A neural circuitry that emphasizes spinal feedback generates diverse behaviours of human locomotion. *The Journal of Physiology*. 2015;593(16):3493-511.
21. Cavagna GA, Heglund NC, Taylor CR. Mechanical work in terrestrial locomotion: two basic mechanisms for minimizing energy expenditure. *American Journal of Physiology*. 1977;233(5):R243-R61.
22. Kuo AD. The six determinants of gait and the inverted pendulum analogy: A dynamic walking perspective. *Human movement science*. 2007;26(4):617-56.
23. Lee CR, Farley CT. Determinants of the center of mass trajectory in human walking and running. *Journal of Experimental Biology*. 1998;201(21):2935-44.
24. Perry J, K ST, Davids JR. Gait Analysis: Normal and Pathological Function. *Journal of Pediatric Orthopaedics*. 1992;12(6):815.
25. Kuo AD, Donelan JM. Dynamic principles of gait and their clinical implications. *Physical Therapy*. 2010;90(2):157-74.
26. Simon SR, Mann RA, Hagy JL, Larsen LJ. Role of the posterior calf muscles in normal gait. *Journal of bone and joint surgery American volume*. 1978;60(4):465-72.
27. Waters RL, Mulroy S. The energy expenditure of normal and pathologic gait. *Gait & posture*. 1999;9(3):207-31.
28. Jahnsen R, Villien L, Aamodt G, Stanghelle JK, Holm I. Musculoskeletal pain in adults with cerebral palsy compared with the general population. *Journal of rehabilitation medicine*. 2004;36(2):78-84.
29. Opheim A, Jahnsen R, Olsson E, Stanghelle JK. Walking function, pain, and fatigue in adults with cerebral palsy: a 7-year follow-up study.

Developmental medicine and child neurology. 2009;51(5):381-8.

30. Rose J, Gamble JG, Burgos A, Medeiros J, Haskell WL. Energy expenditure index of walking for normal children and for children with cerebral palsy. *Developmental medicine and child neurology*. 1990;32(4):333-40.

31. Wren TA, Rethlefsen S, Kay RM. Prevalence of specific gait abnormalities in children with cerebral palsy: influence of cerebral palsy subtype, age, and previous surgery. *Journal of pediatric orthopedics*. 2005;25(1):79-83.

32. Hicks JL, Schwartz MH, Arnold AS, Delp SL. Crouched postures reduce the capacity of muscles to extend the hip and knee during the single-limb stance phase of gait. *J Biomech*. 2008;41(5):960-7.

33. Andriacchi TP, Andersson GB, Fermier RW, Stern D, Galante JO. A study of lower-limb mechanics during stair-climbing. *Journal of bone and joint surgery American volume*. 1980;62(5):749-57.

34. McFadyen BJ, Winter DA. An integrated biomechanical analysis of normal stair ascent and descent. *J Biomech*. 1988;21(9):733-44.

35. Riener R, Rabuffetti M, Frigo C. Stair ascent and descent at different inclinations. *Gait & posture*. 2002;15(1):32-44.

36. Zachazewski JE, Riley PO, Krebs DE. Biomechanical analysis of body mass transfer during stair ascent and descent of healthy subjects. *Journal of Rehabilitation Research & Development*. 1993;30(4):412-22.

37. Koelewijn AD, Dorschky E, van den Bogert AJ. A metabolic energy expenditure model with a continuous first derivative and its application to predictive simulations of gait. *Computer methods in biomechanics and biomedical engineering*. 2018;21(8):521-31.

38. Guertin P. Central Pattern Generator for Locomotion: Anatomical, Physiological, and Pathophysiological Considerations. *Frontiers in Neurology*. 2013 2013-February-08;3(183).

39. Brown TG. On the nature of the fundamental activity of the nervous

centres; together with an analysis of the conditioning of rhythmic activity in progression, and a theory of the evolution of function in the nervous system. *The Journal of Physiology*. 1914;48(1):18-46.

40. Guertin PA. The mammalian central pattern generator for locomotion. *Brain research reviews*. 2009;62(1):45-56.

41. Philippson M. L'autonomie et la centralisation dans le système nerveux des animaux: étude de physiologie expérimentale et comparée: Falk; 1905.

42. Sherrington CS. Flexion-reflex of the limb, crossed extension-reflex, and reflex stepping and standing. *The Journal of Physiology*. 1910;40(1-2):28-121.

43. Gossard JP, Brownstone RM, Barajon I, Hultborn H. Transmission in a locomotor-related group Ib pathway from hindlimb extensor muscles in the cat. *Experimental Brain Research*. 1994;98(2):213-28.

44. Guertin P, Angel MJ, Perreault MC, McCrea DA. Ankle extensor group I afferents excite extensors throughout the hindlimb during fictive locomotion in the cat. *The Journal of Physiology*. 1995;487(1):197-209.

45. MATTHEWS PBC. Mammalian Muscle Receptors and their Central Actions. *American Journal of Physical Medicine & Rehabilitation*. 1974;53(3):143-4.

46. Pearson KG. Proprioceptive regulation of locomotion. *Current opinion in neurobiology*. 1995;5(6):786-91.

47. Stein RB, Capaday C. The modulation of human reflexes during functional motor tasks. *Trends in neurosciences (Regular ed)*. 1988;11(7):328-32.

ABSTRACT (IN KOREAN)

젊은 비장애인 성인에서 내측 비복근의
신경 차단 후 보행 적응

<지도교수 나동욱>

연세대학교 대학원 의학과

성 명 박동호

선행 연구들에서는 비복근 (GCM)의 내측 및 외측의 기능 및 활동을 하나의 근육 단위로서 분석 하였는데, 이는 인체 내에서 각 근육의 기능을 독립적으로 분석하는 것이 기술적으로 어렵기 때문이다. 그러나 비복근의 내측과 외측의 해부학적 차이로 인해 두 근육 간의 기능적 차이가 존재할 것이라 예상된다.

내측 비복근의 독립적인 기능을 알기 위해, 미용목적으로 경골 신경의 분지 중 내측 비복근으로 정지하는 신경 차단술을 받는 젊은 비장애인 성인을 대상으로 평지 및 계단을 보행하는 동안 보행 운동학 및 하지 주요 근육의 근활성도 변화를 실험 및 근골격계 모델을 기반으로 한 예측 시뮬레이션 환경에서

분석하였다.

평지 보행에서 신경 차단술로 인해 내측 비복근의 근활성도가 감소되었고, 내측 비복근의 마비는 보행 시 관절각도를 통계적으로 유의미하게 변화시키지 않았다. 반면, 외측 비복근 및 햄스트링의 근활성도가 통계적으로 유의미하게 증가하였다. 계단을 오르는 보행에서는 내측 비복근의 근활성도가 감소되었고, 평지 보행에서의 결과와는 반대로 내측 비복근의 마비는 보행 시 입각기 (stance phase)의 말기와 입각기에서 유각기로 전환하는 (push-off) 시기에 발목의 족저굴곡 (plantarflexion) 각도를 통계적으로 유의미하게 감소시켰다.

본 연구의 결과를 통해 내측 비복근 마비 시 이에 대응하는 인체의 보행 적응이 보행의 유형에 따라 다르게 나타난다는 사실을 유추 할 수 있다.

핵심되는 말 : 비복근, 보행 적응, 보행 분석, 예측 시뮬레이션, 근골격 모델

PUBLICATION LIST

1. Park D, Seong YJ, Woo H, Yoo B, Shim D, Kim ES, et al. Paralysis of the gastrocnemius medial head differentially affects gait patterns and muscle activity during level and stair ascent locomotion. *Gait Posture*. 2019 Jul;72:222-7.